Sum Rate Maximization for 6G Beyond Diagonal RIS-Assisted Multi-Cell Transportation Systems

Chi Zhang, *Member, IEEE*, Wali Ullah Khan, *Member, IEEE*, Ali Kashif Bashir, *Senior Member, IEEE*, Ashit Kumar Dutta, Ateeq Ur Rehman, *Senior Member, IEEE*, and Maryam M. Al Dabel

***Abstract*— With the rapid evolution toward data-intensive applications and sustainable urban mobility, upcoming sixth-generation (6G) wireless networks must deliver enhanced coverage, high spectral efficiency, and energy optimization across densely populated areas. However, achieving these requirements poses significant challenges due to the dynamic nature of urban environments, high interference in multi-cell systems, and limitations in conventional passive beamforming technologies. To address these challenges, reconfigurable intelligent surface (RIS) is considered a highly promising approach for enabling and improving 6G wireless communications. This is because it has the ability to efficiently manipulate wireless channels at a lower cost. Considerable study has focused on the utilization of conventional diagonal RIS, in which each individual RIS component is linked to its own ground load but not interconnected with other elements. Nevertheless, the uncomplicated structure of classical RIS imposes restrictions on its ability to manipulate passive beamforming. In this study, we consider beyond diagonal RIS (BD-RIS) in the multi-cell transportation system, which goes beyond using diagonal phase shift matrices. In particular, we provide a new optimization framework to maximize the sum rate of BD-RIS assisted multi-cell transportation system by optimizing the power allocation of the base station and phase shift design of BD-RIS in each cell. We employ the block coordinate descent method to transform the original optimization problem and achieve a local optimal based on standard convex approaches. Numerical results demonstrate the benefits of adopting BD-RIS in multi-cell transportation systems compared to the classical RIS architecture.**

***Index Terms*— 6G, beyond diagonal reconfigurable intelligent surfaces, transportation systems, sum rate optimization.**

This work was supported in part by the Science and Technology Research Project of Jiangxi Provincial Department of Education under Grant GJJ211611 and Grant GJJ211608; in part by the National Natural Science Foundation of China under Grant 62261056; in part by the Researchers Supporting Project through Almaarefa University, Riyadh, Saudi Arabia, under Grant MHIRSP2024005. The Associate Editor for this article was V. Menon. *(Corresponding authors: Chi Zhang; Ateeq Ur Rehman.)*

Chi Zhang is with the College of Physical Science and Technology, Yichun University, Yichun, Jiangxi 336000, China (e-mail: 381152345@qq.com).

Wali Ullah Khan is with the Interdisciplinary Centre for Security, Reliability and Trust (SnT), University of Luxembourg, 1855 Luxembourg City, Luxembourg (e-mail: waliullah.khan@uni.lu).

Ali Kashif Bashir is with the Department of Computing and Mathematics, Manchester Metropolitan University, M15 6BX Manchester, U.K., and also with the Centre for Research Impact and Outcome, Chitkara University Institute of Engineering and Technology, Chitkara University, Rajpura, Punjab 140401, India (e-mail: dr.alikashif.b@ieee.org).

Ashit Kumar Dutta is with the Department of Computer Science and Information Systems, College of Applied Sciences, AlMaarefa University, Riyadh 13713, Saudi Arabia (e-mail: adotta@um.edu.sa).

Ateeq Ur Rehman is with the School of Computing, Gachon University, Seongnam-si 13120, Republic of Korea (e-mail: 202411144@gachon.ac.kr).

Maryam M. Al Dabel is with the Department of Computer Science and Engineering, College of Computer Science and Engineering, University of Hafr Al Batin, Hafar Al Batin 39524, Saudi Arabia (e-mail: maldabel@uhb.edu.sa).

I. Introduction

In THE future sixth generation (6G) and beyond wireless networks, the transportation system can enhance connectivity and support high-data-rate services in a vast number of applications [1], [2]. Integrating 6G and beyond with transportation systems will allow efficient management of data from various nodes on the roadside. This integration will also promote sustainable and green mobility solutions [3]. 6G will support low-emission and eco-friendly transportation systems by introducing various emerging technologies. The initial five generations of wireless networks have been managed by adapting to the unpredictable wireless environment using advanced designs at the transmitter and receiver [4]. For sixth-generation and beyond wireless networks, there is an anticipated use of an emerging technology called reconfigurable intelligent surface (RIS) [5]. This technology allows for the modification of both the transceiver and the wireless environment, offering promising advancements in 6G wireless networks. RIS system is composed of many passive phase shift elements, which enable it to alter the wireless environment and thereby improve the spectrum and energy efficiency of the wireless network [6]. The benefits of RIS technology have been proven in many wireless systems, such as cognitive radio networks, device-to-device communication, satellite communication, unmanned aerial vehicles, multi-cell wireless systems, integrated sensing and communication, terahertz communication, vehicular communication, and multiple-input multiple-output [7], [8].

The majority of current research focuses on utilizing a traditional RIS model with a diagonal phase shift matrix, also known as classical RIS [9]. In this model, each phase shift element is linked to its own adaptable impedance without any connections with other phase shift elements on the surface [10]. To be more precise, there are two constraints associated with the classical version of RIS. The first constraint is that the classical diagonal RIS is only able to manipulate the phase of the incoming signal [11]. This limitation restricts its ability to regulate passive beamforming, resulting in a

TABLE I
List of Abbreviations and Notations

Symb./Abbr.	Description
6G	Sixth Generation
BD-RIS	Beyond Diagonal Reconfigurable Intelligent Surface
BS	Base Station
IoT	Internet of Things
LoS	Line of Sight
RIS	Reconfigurable Intelligent Surface
SCA	Successive Convex Approximation
SINR	Signal-to-Interference-Plus-Noise Ratio
STAR-RIS	Simultaneous Transmission and Reflection RIS
B	Number of Base Stations
K	Number of Vehicular Users
N	Number of Resource Blocks
M	Number of BD-RIS Elements
$\mathcal{B}$	Set of Base Stations
$\mathcal{K}$	Set of Vehicular Users
$\mathcal{N}$	Set of Resource Blocks
$g_{b,k,n}$	Channel from BS to Vehicular User (Direct Link)
$h_{b,k,n}$	Channel from BS to BD-RIS
$f_{b,k,n}$	Channel from BD-RIS to Vehicular Users
$p_{b,k,n}$	Power Allocation for BS to User over Resource Block
$\mathbf{\Phi}$	Scattering Phase Shift Matrix of BD-RIS
$\gamma_{b,k,n}$	Signal-to-Interference-Plus-Noise Ratio
σ^2	Variance of Additive White Gaussian Noise
R_{sum}	Achievable Sum Rate

degradation of performance. The second constraint is that it exclusively facilitates signal reflection in the same direction, hence restricting the coverage [12]. In means that the transmitter and receiver should be in front of the classical RIS.

In order to overcome the constraints of classical diagonal RIS and improve the performance of this emerging technology, this work introduces beyond diagonal RIS (BD-RIS) [13]. This new version of the RIS family incorporates inter-element connections, which, although increasing circuit complexity, significantly improves system performance [14]. The mathematical model of BD-RIS is not restricted to diagonal matrices, it offers a full scattering phase shift matrix where different phase shift elements are interconnected [15]. In this work, we assess the attainable sum-rate performance of BD-RIS assisted multi-cell system with inter-cell interference using optimal power allocation and phase shift design. All the abbreviations and notations used in this work are defined in Table I. To better understand BD-RIS, we discuss its operating modes, hardware architectures, and advantages.

A. Modes of BD-RIS Technology

This new model of reconfigurable technology can operate in three modes: reflective mode, transmissive mode, and hybrid mode [16].

1) Reflective BD-RIS: This mode of BD-RIS technology primarily emphasizes modifying the phase and maybe the amplitude of electromagnetic waves that are reflected by the reconfigurable surface [17]. It is crucial in situations when it is necessary to alter the signal flow, such as in locations where impediments obstruct direct line-of-sight transmission. This mode of BD-RIS technology guarantees the efficient redirection of signals to their designated destination. The phase shift matrix of reflective BD-RIS can be described as $\mathbf{\Phi}_r^H\mathbf{\Phi}_r = \mathbf{I}_M$, where $\mathbf{I}_M$ shows the identity matrix.

2) Transmissive BD-RIS Technology: Unlike the reflecting mode of BD-RIS technology, the transmissive mode of the BD-RIS permits electromagnetic impulses to flow through the surface, while undergoing changes. The transmissive BD-RIS technology is beneficial in environments where the reconfigurable surface is integrated into translucent structures, such as glass walls or barriers [18]. By doing this, the transmissive BD-RIS functions as a structural component and actively engages in the communication process by modifying the signals that traverse it. When BD-RIS operates in transmissive mode, its phase shift matrix can defined as $\mathbf{\Phi}_t^H\mathbf{\Phi}_t = \mathbf{I}_M$.

3) Hybrid BD-RIS Technology: The hybrid mode of BD-RIS technology combines the functionalities of both the reflecting and transmissive modes. BD-RIS operating in this mode has the ability to reflect and transmit signals at the same time, making it a versatile option for complex communication contexts [19]. The BD-RIS operating in hybrid mode is also called STAR-RIS when the reconfigurable elements are not inter-connected (also called single-connected). The hybrid mode emphasizes the importance of adaptability in situations when various signal manipulation is needed to enhance network coverage and efficiency. The phase shift matrices of this mode can be expressed as $\mathbf{\Phi}_r^H\mathbf{\Phi}_r + \mathbf{\Phi}_t^H\mathbf{\Phi}_t = \mathbf{I}_M$.

B. Hardware Architectures of BD-RIS Technology

The architecture of BD-RIS technology can be classified into three types: single-connected BD-RIS technology, fully-connected BD-RIS technology, and group-connected BD-RIS technology, as illustrated in Fig. 1.

1) Single-Connected BD-RIS Technology: This architecture is the most basic and essential one of the BD-RIS technology. Each reconfigurable element in the single-connected architecture of BD-RIS technology operates independently, with its main objective being the alteration of the phase of the electromagnetic waves that are received [20]. The design is commonly depicted using a diagonal matrix arrangement, where each diagonal element independently regulates the phase shift of a corresponding RIS element, without any interactions between the elements. All matrices in this architecture are diagonal.

2) Fully-Connected BD-RIS Technology: The fully-connected impedance network interconnects every element inside the BD-RIS system, as the design complexity increases. This advanced architecture setup provides a high level of control over electromagnetic signals, allowing for precise changes in both their phase and magnitude [21]. The increased level of interconnectedness in fully-connected architecture results in improved overall functionality, greatly enhancing the RIS's ability to strengthen and alter signals. In fully-connected BD-RIS, all the matrices are full.

3) Group-Connected BD-RIS Technology: The group-connected architecture of BD-RIS is a system that combines the simplicity of a single connected network with the complexity of a fully connected network [22]. It arranges the BD-RIS

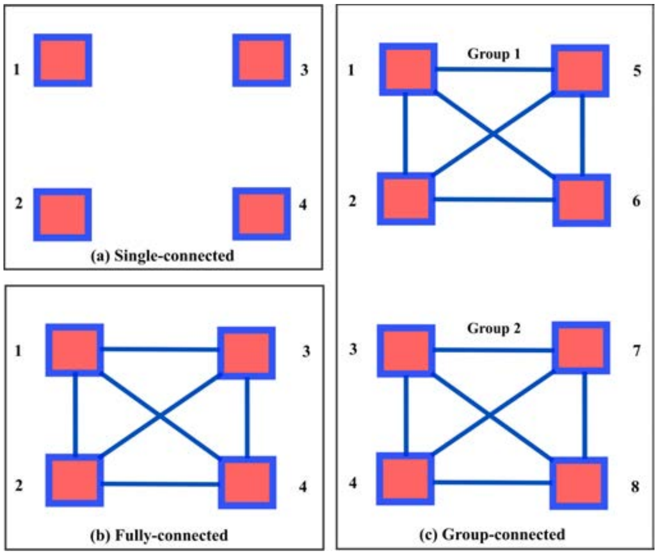

Fig. 1. Different architectures of BD-RIS technology: (a) Single-connected BD-RIS technology, (b) Fully-connected RIS technology, and (c) Group-connected BD-RIS technology.

technology into separate groups on the same surface. Each reconfigurable element inside the same group is interconnected and forms a fully-connected architecture. This architectural design achieves a practical equilibrium by providing sophisticated wave manipulation abilities while also minimizing the overall complexity of the system. In the group-connected architecture of BD-RIS technology, each group provides full matrices while the whole surface provides block diagonal matrices.

C. Advantages of BD-RIS Technology

Compared to the classical RIS technology, BD-RIS technology offers the following advantages.

1) Improved System Efficiency: One of the advantages of BD-RIS technology is that it exhibits a significant enhancement in performance when compared to classical diagonal RIS technology, especially in terms of signal strength and overall network efficiency. The improved performance is essential for enhancing the quality and dependability of future wireless communications, presenting BD-RIS as a vital technology for the future of communication networks. The ability to precisely manipulate electromagnetic waves greatly expands the possibilities of wireless technology.

2) Enhanced Received Signal Power: Another significant benefit of BD-RIS technology, particularly in its fully-connected architecture and group-connected setups, is the substantial improvement in the strength of received signals. This enhancement greatly exceeds the capabilities of single-connected BD-RIS architecture, resulting in a significant enhancement in the efficiency of wireless communication systems. The capacity of BD-RIS to increase signal strength is crucial in improving the range, coverage, and reliability of communication networks.

3) Flexible System Deployment: The range of architectural designs offered by BD-RIS technology allows for great adaptability, making it highly suitable for a wide range of communication settings. The capacity to adapt is crucial for customizing network infrastructure to operate at its best in many situations, ranging from highly populated urban regions to expansive rural landscapes. Moreover, BD-RIS technology offers network operators the ability to tailor the technology to address specific environmental and communication hurdles.

II. Recent Advances and Our Contributions

In this section, we first discuss the recent advances in this research area and then we make motivation and contributions.

A. Recent Advances in RIS Assisted Vehicular Networks

Most of the existing literature has considered conventional diagonal RIS in different wireless scenarios. For instance, Zhao et al. [23] have employed a deep reinforcement learning based optimization approach for data rate maximization in RIS assisted unmanned aerial vehicle (UAV) communication. In [24], the authors have proposed a digital twin enabled RIS assisted UAV communication to minimize the transmission power consumption of the system. Moreover, Ji et al. [25] have proposed two communication scenarios of RIS-relay assisted RIS equipped source and relay assisted RIS equipped source in vehicular communication and investigated system outage probability. In [26], authors have explored the closed-form expression of outage probability and bit error rate in RIS assisted vehicular networks. Shang et al. [27] have proposed a secure communication network in index modulation based RIS assisted vehicular network. Furthermore, the authors of [28] have studied a problem of physical layer security in RIS assisted vehicular communication with multiple eavesdroppers. Of late, Ji et al. [29] have considered task offloading and resource allocation problem in RIS assisted vehicular communication networks.

Recently, researchers in academia and industry have considered BD-RIS in their proposed works. The authors of [30] have proposed a framework of transmit precoding and phase shift design in BD-RIS assisted multi-user wireless networks. In [14], a closed-form expression is derived to improve the average received signal and achievable rate of BD-RIS assisted wireless networks. In [31], the same authors have optimized the phase response in multi-antenna and single-antenna scenarios to maximize the received power of a multi-user system. Moreover, the work in [32] has proposed a mutual coupling aware optimization framework to maximize the channel gain of BD-RIS system. Sun et al. [33] have proposed as optimization framework to investigate different performance metrics in BD-RIS assisted wireless systems. Besides that, the work in [34] has also considered BD-RIS as a transmitter in order to assess the system performance. Furthermore, the authors of [35] have provided a power minimization approach for BD-RIS assisted integrated sensing and communication. Fang and Mao [36] have investigated the spectral efficiency of multi-user in BD-RIS assisted wireless networks. Off late, Li et al. [37] have investigated the power gain of BD-RIS assisted wireless system.

B. Motivation and Our Contributions

It is important to note that the research on BD-RIS is in the initial stage and there exists many open problems that need to be investigated. Motivated by this, we consider BD-RIS in transportation systems which has not been studied previously in the literature. Considering the existing literature, this is the first work on BD-RIS assisted transportation systems. In particular, we maximize the sum rate of the multi-cell transportation system by optimizing the power allocation and phase shift design. The original joint optimization problem is complex and obtaining an optimal joint solution is challenging. To make the sum rate maximization problem tractable, we first split it into two problems by adopting the block coordinate descent (BCD) method. By using this method, the original joint problem is transformed into a power allocation problem and a phase shift problem. Then, these problems are further transformed into linear problems, and local optimal solutions are achieved through standard convex optimization methods. To analyze the performance of the proposed BD-RIS assisted transportation system, we consider traditional diagonal RIS (TD-RIS), simultaneous transmission and reflection RIS (also called STAR RIS) as the benchmark optimization frameworks. Our main contribution can be summarized as follows.

1) This work considers a BD-RIS assisted transportation scenario, wherein each cell, a base station (BS) performs downlink transmission with K vehicular users using N resource blocks. To enhance the spectral efficiency of the system, we consider that all the BSs reuse the same resource blocks. Hence, each BS receives interference from neighboring BSs and causes interference to the neighboring cell's vehicular users. Moreover, we are considering the urban area where line of sight (LoS) links between BSs and their serving vehicular users cannot be guaranteed all the time, and vehicular users can face large-scale fading and blockages due to the neighboring obstacles.
2) To enhance the received signal strength and ensure smooth connectivity between BSs and vehicular users, we consider that BD-RIS is mounted in the optimal position in each cell, which delivers signals from BS to vehicular users. Therefore, vehicular users receive signals from direct links as well as BD-RIS assisted links. The objective of the proposed scenario is to improve the spectral efficiency of the system by optimizing the power allocation and phase shift design while ensuring the minimum rate constraint of vehicular users in each cell. Due to the coupled variables and inter-cell interference, the joint optimization problem for sum rate maximization is formulated as a mixed integer non-linear programming problem.
3) The original joint optimization problem is complex and obtaining an optimal joint solution is challenging. To make the sum rate maximization problem tractable, we first split it into two problems by adopting the BCD method. By using this method, the original joint problem is transformed into a power allocation problem and a phase shift problem. Then, these problems are further transformed into linear problems, and local optimal solutions are achieved through standard convex optimization methods. To analyze the performance of the proposed BD-RIS assisted transportation system, we consider classical RIS, simultaneous transmission, and STAR RIS as the benchmark optimization frameworks.

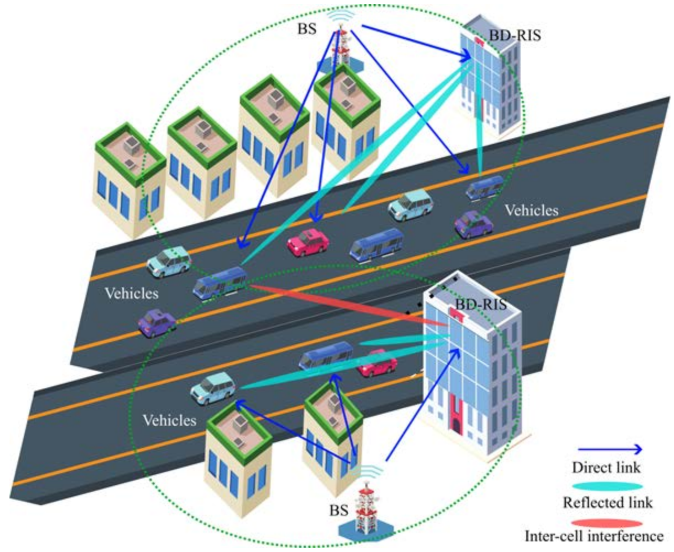

Fig. 2. System model.

The remaining of this work is structured as follows. In Section III, we discuss the considered scenario, channel modeling, and problem formulation. In Section IV, we provide the details of the proposed solution. In Section V, we present and discuss the numerical results. In Section VI, we finalize our work with concluding remarks.

III. System Model and Problem Formulation

Let us consider a downlink multi-cell transportation scenario where B BSs communicate with their K associated vehicular users using N resource blocks, as illustrated in Fig. 2. The set of BSs and vehicular users and resource blocks can be defined as $\mathcal{B} = \{b|1, 2, 3, \ldots, B\}$, $\mathcal{K} = \{k|1, 2, 3, \ldots, K\}$, and $\mathcal{N} = \{n|1, 2, 3, \ldots, N\}$, respectively. To maximize the spectral efficiency of the system, each BS reuses all resource blocks; hence, neighboring BSs cause cochannel interference with each other [38]. This work examines a communication scenario in a smart city, where it is not always possible to guarantee direct links between BSs and vehicular users due to blockages and vehicular user's mobility. To tackle this problem, a BD-RIS is installed in the optimal position in the coverage of each cell to assist the communication between BS and vehicular users[1] Each BD-RIS consists of M reconfigurable elements, described as $\mathcal{M} = \{m|1, 2, 3, \ldots, M\}$. We assume that the BSs have complete knowledge of the

[1]This work considers a reflective mode of BD-RIS that is efficient in outdoor communication scenarios. Operating BD-RIS in hybrid mode can be effective when considering both indoor and outdoor communication scenarios at the same time. However, this is outside the scope of this study.

channel state information of all associated vehicular users, and channel acquisition can be achieved through channel estimation techniques prior to the communication process.

The channel from BS to the vehicular user (direct link), from BS to BD-RIS, and from BD-RIS to vehicular users over n-th resource block in b-th cell can be modeled as $g_{b,k,n}$, $h_{b,k,n}$, and $f_{b,k,n}$, where $l_{b,k,n} = \bar{l}_{b,k,n} d_{b,k,n}^{-\alpha/2}$, $l \in \{g, h, f\}$ [39]. Here $l \sim \mathcal{CN}(0, \sigma^2)$ states the Rayleigh fading coefficient, d is the distance between two terminals in the cell, and α denotes the path loss. The signal that b-th BS transmits to k-th vehicular user over n-th resource block can be expressed as $\sqrt{p_{b,k,n}} x_{b,k,n}$, where $p_{b,k,n}$ is the allocated power of BS for k-th vehicular user over n-th resource block, and $x_{b,k,n}$ shows the unit power signal of k-th vehicular user over n-th resource block. The signal that the k-th vehicular user receives from the b-th BS over the n-th resource block through a direct and BD-RIS assisted link can be written as:

$$\begin{aligned} y_{b,k,n} &= \underbrace{\sum_{k=1}^{K}\sum_{n=1}^{N}(g_{b,k,n} + \mathbf{h}_{b,k,n}\mathbf{\Phi}\mathbf{f}_{b,k,n})x_{b,k,n}}_{\text{desired signal}} + \underbrace{\omega_{b,k,n}}_{\text{AWGN}} \\ &+ \underbrace{\sum_{b'=1,b'\neq b}^{B}\sum_{k'=1}^{K}\sum_{n'=1}^{N}(g_{b',k',n'} + \mathbf{h}_{b',k',n'}\mathbf{\Phi}\mathbf{f}_{b',k',n'})x_{b',k',n'}}_{\text{inter-cell interference}}, \end{aligned} \tag{1}$$

where $\mathbf{h}_{b,k,n}, \mathbf{h}_{b',k',n'} \in M \times 1$ and $\mathbf{f}_{b,k,n}, \mathbf{f}_{b',k',n'} \in 1 \times M$ while $n_{b,k,n}$ is the additive white Gaussian noise (AWGN) with zero means and σ^2 variance. Moreover, $\mathbf{\Phi} \in M \times M$ denotes the scattering matrix of BD-RIS such that $\mathbf{\Phi}\mathbf{\Phi}^H = \mathbf{I}_K$. Based on the received signal derived in (1), the rate of k-th vehicular user from b-th BS over n-th resource block can be defined as $R_{b,k,n} = \log_2(1 + \gamma_{b,k,n})$, where $\gamma_{b,k,n}$ is the signal to interference plus noise ratio and can be expressed as:

$$\gamma_{b,k,n} = \frac{|g_{b,k,n} + \mathbf{H}|^2 p_{b,k,n}}{\sum_{b'=1}^{B}\sum_{k'=1}^{K}\sum_{n'=1}^{N}|g_{b',k',n'} + \mathbf{H}'|^2 p_{b',k',n'} + \sigma^2} \tag{2}$$

where $\mathbf{H} = \mathbf{h}_{b,k,n}\mathbf{\Phi}\mathbf{f}_{b,k,n}$ and $\mathbf{H}' = \mathbf{h}_{b',k',n'}\mathbf{\Phi}\mathbf{f}_{b',k',n'}$. The term in the denominator represents the inter-cell interference. Cindering the B cells, the achievable sum rate of the entire transportation can be derived as:

$$R_{sum} = \sum_{b=1}^{B}\sum_{k=1}^{K}\sum_{n=1}^{N}\log_2(1 + \gamma_{b,k,n}), \tag{3}$$

This work aims to maximize the achievable sum rate of BD-RIS assisted multi-cell transportation by optimizing the power allocation of BS and phase shift of BD-RIS in each cell subject to minimum vehicular user data rate.[2] The problem of maximizing the sum rate can be formulated as:

$$2(P): \begin{cases} \max\limits_{(p_{b,k,n},\mathbf{\Phi})} \; R_{sum} \\ \mathcal{C}_1: \sum_{b=1}^{B}\sum_{k=1}^{K}\sum_{n=1}^{N} R_{b,k,n} \geq R_{min}, \\ \mathcal{C}_2: \sum_{b=1}^{B}\sum_{k=1}^{K}\sum_{n=1}^{N} p_{b,k,n} \leq P_{tot}, \\ \mathcal{C}_3: \mathbf{\Phi}\mathbf{\Phi}^H = \mathbf{I}_K \end{cases} \tag{4}$$

where constraint $\mathcal{C}_1$ ensures the minimum data rate of vehicular users in each cell and R_{min} is the minimum threshold. Constraint $\mathcal{C}_2$ limits the transmit power of BS in each cell, where P_{tot} is the total power budget of BS. Constraint $\mathcal{C}_3$ controls the phase shift of BD-RIS in each cell.

The optimization problem (4) is classified as a mixed-integer nonlinear due to the logarithmic function present in the rate equation [40], [41]. Furthermore, the unitary constraint C_3 makes it NP-hard. As a result, obtaining the optimal solution requires significant computational effort. To address this, the following section introduces the use of the BCD method, which simplifies the original optimization problem into multiple sub-problems, thereby facilitating the finding of the local optimal solution for the joint optimization problems. Additionally, the sub-optimization problem is solved through iterative methods.

IV. Proposed Scheme

In this section, we discuss the utilization of the BCD method to partition the joint optimization problem into two categories: the power allocation set $\{p_{b,k,n}\}$ and the BD-RIS phase shifts $\mathbf{\Phi}$. This partitioning aids in overcoming the coupling of the decision variables. The BCD method alternately optimizes one category while keeping the other fixed. Additionally, to address the nonlinearity and non-convexity related to their respective decision variables, these subproblems are transformed into linear forms, making them suitable for solving using the standard MATLAB convex optimization toolbox.

A. Power Allocation Subproblem

The power allocation subproblem aims to optimize the power allocation $\{p_{b,k,n}\}$ while keeping the BD-RIS phase shifts $\mathbf{\Phi}$ fixed. The subproblem is formulated as follows:

$$(P1): \begin{cases} \max\limits_{p_{b,k,n}} R_{sum} \\ \mathcal{C}_1: \sum_{b=1}^{B}\sum_{k=1}^{K}\sum_{n=1}^{N} R_{b,k,n} \geq R_{min}, \\ \mathcal{C}_2: \sum_{b=1}^{B}\sum_{k=1}^{K}\sum_{n=1}^{N} p_{b,k,n} \leq P_{tot}. \end{cases} \tag{5}$$

The optimization problem (5) continues to be nonlinear because of the logarithmic function in the rate equation included in both the objective function and the constraint C_1. To address this issue, we utilize the Successive Convex

[2] In this work, we assume that the assignment of resource blocks to vehicular users has already been done before the optimization process. The optimal resource block assignment may further improve the system performance, however, it is beyond the scope of this work.

Approximation (SCA) method to transform the rate equation into a linear form. The rate $R_{b,k,n}$ is expressed as:

$$R_{b,k,n} = \log_2\left(1 + \gamma_{b,k,n}\right), \tag{6}$$

where $\gamma_{b,k,n}$ in (6) denotes the SINR, defined as:

$$\gamma_{b,k,n} = \frac{|g_{b,k,n} + \mathbf{H}|^2 p_{b,k,n}}{\sum_{b'=1, b'\neq b}^{B} \sum_{k'=1}^{K} \sum_{n'=1}^{N} |g_{b',k',n'} + \mathbf{H}'|^2 p_{b',k',n'} + \sigma^2}. \tag{7}$$

To handle the non-linear term, we define the (6) as a function of $\gamma_{b,k,n}$, represented as $f(\gamma_{b,k,n}) = \log_2(1+\gamma_{b,k,n})$. We then apply the first-order Taylor expansion at the feasible point $p_{b,k,n}^{(t)}$ during iteration t and can be expressed as:

$$f(\gamma_{b,k,n}) \approx f(\gamma_{b,k,n}^{(t)}) + f'(\gamma_{b,k,n}^{(t)})(\gamma_{b,k,n} - \gamma_{b,k,n}^{(t)}). \tag{8}$$

where $f'(\gamma_{b,k,n}^{(t)})$ is the derivative of $f(\gamma_{b,k,n})$ with respect to $\gamma_{b,k,n}$, evaluated at $\gamma_{b,k,n}^{(t)}$:

$$f'(\gamma_{b,k,n}) = \frac{1}{\ln(2)(1+\gamma_{b,k,n})}. \tag{9}$$

Hence, the approximated rate equation can be formulated as:

$$R_{b,k,n} \approx \log_2(1+\gamma_{b,k,n}^{(t)}) + \frac{1}{\ln(2)(1+\gamma_{b,k,n}^{(t)})}(\gamma_{b,k,n} - \gamma_{b,k,n}^{(t)}). \tag{10}$$

Substituting $\gamma_{b,k,n}$, in (8) we get (11).

$$\gamma_{b,k,n} \approx \gamma_{b,k,n}^{(t)} + \frac{|g_{b,k,n} + \mathbf{H}|^2}{\sum_{b'=1, b'\neq b}^{B} \sum_{k'=1}^{K} \sum_{n'=1}^{N} |g_{b',k',n'} + \mathbf{H}'|^2 p_{b',k',n'} + \sigma^2} \times \left(p_{b,k,n} - p_{b,k,n}^{(t)}\right). \tag{11}$$

Likewise, by integrating equations (11) and (10), the estimated rate is formulated as

$$R_{b,k,n} \approx \log_2(1+\gamma_{b,k,n}^{(t)}) + \frac{1}{\ln(2)(1+\gamma_{b,k,n}^{(t)})} \times \frac{|g_{b,k,n} + \mathbf{H}|^2}{\sum_{b'=1, b'\neq b}^{B} \sum_{k'=1}^{K} \sum_{n'=1}^{N} |g_{b',k',n'} + \mathbf{H}'|^2 p_{b',k',n'} + \sigma^2} \times \left(p_{b,k,n} - p_{b,k,n}^{(t)}\right). \tag{12}$$

Up to now, the rate equations have been linear with respect to $p_{b,k,n}$, leading to the alteration of constraint C_1 into $\mathcal{C}_1'$, which is mathematically formulated as (13), shown at the bottom of the next page.

Therefore, the transformed subproblem $(P1')$ is:

$$(P1') : \begin{cases} \max_{p_{b,k,n}} \sum_{b=1}^{B} \sum_{k=1}^{K} \sum_{n=1}^{N} \left(R_{b,k,n}\right) \\ \mathcal{C}_1' : (13) \\ \mathcal{C}_2 : \sum_{b=1}^{B} \sum_{k=1}^{K} \sum_{n=1}^{N} p_{b,k,n} \leq P_{tot}. \end{cases} \tag{14}$$

However, after transformation, problem $(P1')$ exhibits both convexity and linearity, allowing it to be addressed through conventional convex optimization methods such as CVX. Moreover, the detailed explanation and working principle are illustrated in Algorithm 1

Algorithm 1 Power Allocation Optimization

Input: Initial power allocation $\{p_{b,k,n}^{(0)}\}$, phase shifts $\mathbf{\Phi}$, tolerance ϵ
Output: Optimized power allocation $\{p_{b,k,n}^{*}\}$

Initialization: Set iteration count $t = 0$ and $\{p_{b,k,n}^{(t)}\}$.
repeat
- **Step 1: Compute SINR approximation**
  Compute $\gamma_{b,k,n}^{(t)}$ using $\{p_{b,k,n}^{(t)}\}$:
- **Step 2: Compute Rate Approximation**
  Approximate $R_{b,k,n}$: using Eq. (12)
- **Step 3: Update Power Allocation**
  Solve the following optimization problem to update $\{p_{b,k,n}\}$: using Eq. (14)
- **Step 4: Check Convergence**
  If $\|\{p_{b,k,n}^{(t+1)}\} - \{p_{b,k,n}^{(t)}\}\| \leq \epsilon$, **stop** the iteration.
- **Step 5: Update Iteration Count**
  Set $t = t + 1$.

until $\|\{p_{b,k,n}^{(t+1)}\} - \{p_{b,k,n}^{(t)}\}\| \leq \epsilon$;
Output: Optimized power $\{p_{b,k,n}^{*} = p_{b,k,n}^{(t+1)}\}$.

B. BD-RIS Phase Shifts Subproblem

With the optimized and constant power allocation $\{p_{b,k,n}\}$, the mathematical formulation of the subproblem for optimizing the BD-RIS phase shifts $\mathbf{\Phi}$ is as follows:

$$(P2) : \begin{cases} \max_{\mathbf{\Phi}} \sum_{b=1}^{B} \sum_{k=1}^{K} \sum_{n=1}^{N} \left(R_{b,k,n}\right) \\ \mathcal{C}_3 : \mathbf{\Phi}\mathbf{\Phi}^H = \mathbf{I}_K. \end{cases} \tag{15}$$

The optimization problem (15) remains NP-hard and non-convex due to the unitary constraint $\mathcal{C}_3$, which makes it computationally difficult to find solutions. To simplify the optimization, we relax the unitary constraint $\mathcal{C}_3$. Instead of strictly enforcing $\mathbf{\Phi}\mathbf{\Phi}^H = \mathbf{I}_K$, we implement a more adaptable constraint that allows the elements of $\mathbf{\Phi}$ to vary within a defined range. This revised constraint is formulated as:

$$\mathcal{C}_3' : \|\mathbf{\Phi}\|_F^2 \leq C, \tag{16}$$

where $\|\cdot\|_F$ represents the Frobenius norm, and C is a constant that limits the norm of $\mathbf{\Phi}$. Furthermore, the transformation of the rate equation remains non-convex due to the phase shift matrix; hence, to tackle this issue, a first-order Taylor expansion is utilized to approximate the non-linear term at a feasible point $\mathbf{\Phi}^{(t)}$ during iteration t. Given that $\gamma_{b,k,n}$ is influenced by $\mathbf{\Phi}$, it is explicitly defined in relation to $\mathbf{\Phi}$ as:

$$\gamma_{b,k,n} \approx \gamma_{b,k,n}^{(t)} + \frac{\Psi_{b,k,n}}{\Omega_{b,k,n}}. \tag{17}$$

where $\Psi_{b,k,n}$ and $\Omega_{b,k,n}$ are specified in (18) and (19), as shown at the bottom of the next page.

Thus, the modified rate equation can be expressed as

$$R_{b,k,n} \approx \log_2(1+\gamma_{b,k,n}^{(t)}) + \frac{1}{\ln(2)(1+\gamma_{b,k,n}^{(t)})} \cdot \frac{\Psi_{b,k,n}}{\Omega_{b,k,n}}. \quad (20)$$

Therefore, by applying the revised rate equation (20), the transformed convex and relaxed optimization problem $(P2')$ is reformulated as:

$$(P2'): \begin{cases} \max\limits_{\mathbf{\Phi}} \sum\limits_{b=1}^{B}\sum\limits_{k=1}^{K}\sum\limits_{n=1}^{N}\left(R_{b,k,n}\right) \\ \mathcal{C}_3': \|\mathbf{\Phi}\|_F^2 \leq C. \end{cases} \quad (21)$$

Therefore, the optimization problem $(P2')$ is now linear and convex, making it simpler to solve by relaxing the unitary constraint. This adjustment aids in solving it using conventional convex optimization methods like CVX. Additionally, a comprehensive explanation and methodological steps are detailed in Algorithm 2.

Algorithm 2 BD-RIS Phase Shifts Optimization

Input: Initial phase shifts $\mathbf{\Phi}^{(0)}$, power allocation $\{p_{b,k,n}\}$, tolerance ϵ

Output: Optimized phase shifts $\mathbf{\Phi}^*$

Initialization: Set iteration count $t = 0$ and $\mathbf{\Phi}^{(t)}$.

repeat

- **Step 1: Compute SINR approximation**
  Compute $\gamma_{b,k,n}^{(t)}$ using $\mathbf{\Phi}^{(t)}$:
  Step 2: Compute Rate Approximation
  Approximate $R_{b,k,n}$: using Eq. (20)
- **Step 3: Update Phase Shifts**
  Solve the following optimization problem to update $\mathbf{\Phi}$: using Eq. (21)
- **Step 4: Check Convergence**
  If $\|\mathbf{\Phi}^{(t+1)} - \mathbf{\Phi}^{(t)}\|_F \leq \epsilon$, **stop** the iteration.
- **Step 5: Update Iteration Count**
  Set $t = t + 1$.

until $\|\mathbf{\Phi}^{(t+1)} - \mathbf{\Phi}^{(t)}\|_F \leq \epsilon$;

Output: Optimized phase shifts $\mathbf{\Phi}^* = \mathbf{\Phi}^{(t+1)}$.

C. Complexity and Convergence Analysis

After computing the proposed solutions in III-A and III-B, in the following, we discuss their complexity and convergence.

1) Complexity Analysis:

- **Optimization of BD-RIS Phase Shifts:** The adjustment of phase shifts $\mathbf{\Phi}$ mainly requires matrix manipulations and tackling the optimization issue in Step 3. The complexity per iteration approximates $O(BKM^2)$, with B denoting the count of base stations, K indicating users per base station, and M representing the BD-RIS elements. The total complexity depends on the number of iterations required for convergence.
- **Power Allocation Optimization:** The process of modifying the power allocation $\{p_{b,k,n}\}$ involves calculating the SINR for each user and addressing the convex optimization problem in Step 3. Each iteration has a complexity of about $O(BKN)$, with N representing the number of resource blocks. The overall complexity depends on the number of iterations required for convergence.

2) Convergence Analysis:

- **BD-RIS Phase Shifts Optimization:** Employing the SCA method for BD-RIS phase shifts optimization guarantees that the objective function value does not decrease through iterations, eventually reaching a local maximum. The rate of convergence is affected by the choice of step size and the initial phase shifts $\mathbf{\Phi}^{(0)}$.
- **Power Allocation Optimization:** In a similar vein, the power allocation optimization employs the SCA approach, guaranteeing that the value of the objective function either increases or stays constant in each iteration. This approach results in a local optimum. The convergence speed is influenced by the initial power configurations $\{p_{b,k,n}^{(0)}\}$ and the predefined tolerance ϵ.
- Both methods utilize the SCA approach, ensuring convergence to a local optimum while maintaining reasonable complexity, taking into account standard values for B, K, N, and M. The convergence behavior is typically stable and predictable, with appropriate initial conditions and step sizes set.

V. Numerical Findings and Analysis

In this section, we present the numerical results to demonstrate the efficacy of the proposed scheme where BD-RIS is utilized to offer services to the user in a multi-cell ITS

$$\sum_{b=1}^{B}\sum_{k=1}^{K}\sum_{n=1}^{N}\left(\log_2(1+\gamma_{b,k,n}^{(t)}) + \frac{1}{\ln(2)(1+\gamma_{b,k,n}^{(t)})}\frac{|g_{b,k,n}+\mathbf{H}|^2}{\sum\limits_{b'=1,b'\neq b}^{B}\sum\limits_{k'=1}^{K}\sum\limits_{n'=1}^{N}|g_{b',k',n'}+\mathbf{H}'|^2 p_{b',k',n'}+\sigma^2} \times \left(p_{b,k,n} - p_{b,k,n}^{(t)}\right)\right) \geq R_{\min}. \quad (13)$$

$$\Psi_{b,k,n} = 2\mathrm{Re}\left[\left(g_{b,k,n} + \mathbf{h}_{b,k,n}\mathbf{\Phi}^{(t)}\mathbf{f}_{b,k,n}\right)^H \mathbf{h}_{b,k,n}(\mathbf{\Phi} - \mathbf{\Phi}^{(t)})\mathbf{f}_{b,k,n}\right] p_{b,k,n}. \quad (18)$$

$$\Omega_{b,k,n} = \sum_{b'=1,b'\neq b}^{B}\sum_{k'=1}^{K}\sum_{n'=1}^{N}|g_{b',k',n'} + \mathbf{h}_{b',k',n'}\mathbf{\Phi}\mathbf{f}_{b',k',n'}|^2 p_{b',k',n'} + \sigma^2. \quad (19)$$

TABLE II
SIMULATION PARAMETERS BASED ON 3GPP STANDARDS

Parameter	Symbol	Value
Carrier Frequency	f_c	2 GHz
Bandwidth	B_w	10 MHz
Number of Base Stations	B	7
Number of Users per BS	K	10
Number of Resource Blocks	N	50
Number of BD-RIS Elements	M	64
Path Loss Exponent	α	3.76
Noise Power Spectral Density	N_0	-174 dBm/Hz
Total Power Budget per BS	P_{tot}	40 dBm
Minimum Rate Requirement	R_{min}	1 Mbps
Reflection Coefficient	β	1
Small-Scale Fading	-	Rayleigh

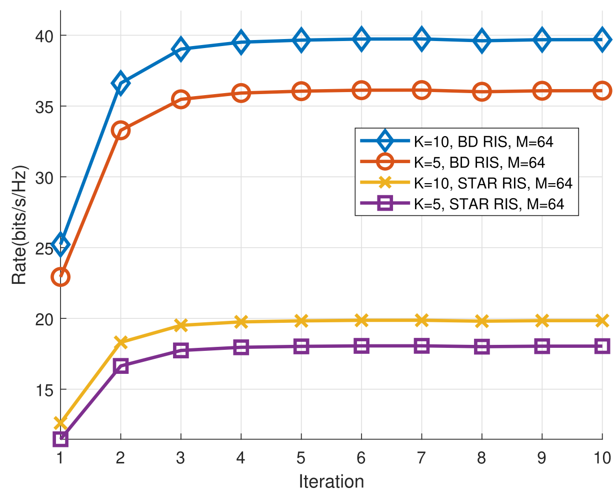

Fig. 3. Number of iterations versus the rate of the proposed transportation system.

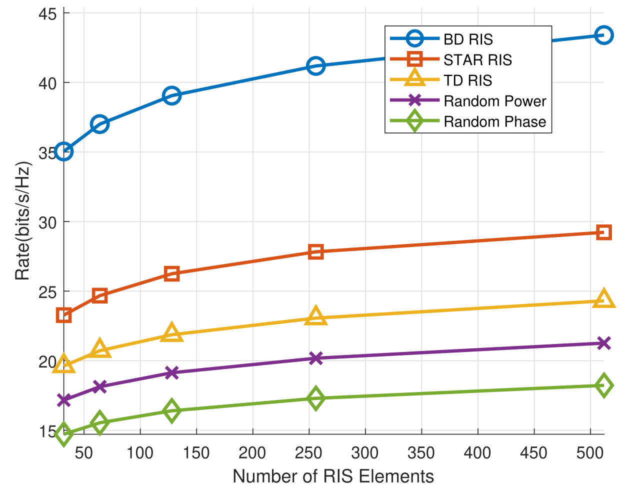

Fig. 4. Number of RIS elements versus the achievable rate of the proposed transportation system.

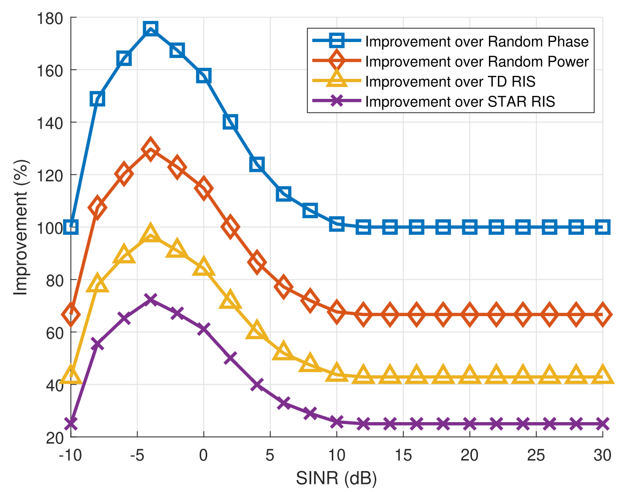

Fig. 5. Percentage improvement of BD-RIS over random phase, random power, TD-RIS, and STAR-RIS schemes across varying SINR levels.

scenario. Extensive simulations were conducted using the simulation parameters listed in Table II. Additionally, to further demonstrate the effectiveness of the proposed scheme, results are compared with key benchmark schemes including TD-RIS [42], STAR RIS [43], and random power and phase shift optimization techniques. Furthermore, extensive Monte Carlo simulations were performed, and average results were generated across independent channel realizations.

A. Results Discussion

Prior to delving into the findings, it is crucial to analyze the convergence of the algorithm. To this end, extensive simulations were conducted, using rate as a performance metric and plotting it against the number of iterations. Simulations considered $K = [5, 10]$, $M = 64$ for both STAR RIS and BD-RIS in Fig. 3. The results indicate that as the number of iterations increases, the algorithm approaches a stable point. Furthermore, the results show that the convergence behavior varies with different simulation parameters. This variation is attributed to the increased computational demand required to reach the local optimal solution for the joint optimization problem described in (4). Additionally, this also validate the convergence analysis conducted in section IV-C.1.

Subsequently, Fig. 4 illustrates the influence of RIS elements on system efficiency with parameters set at $B = 7$, $K = 10$, and $N = 50$. The analysis was conducted over a range of RIS elements, varying M from 32 to 512. Furthermore, these findings were contrasted against pertinent benchmark schemes. The data indicate that an increase in RIS elements enhances system performance, as these elements steer the signal towards specific users, thereby creating an alternative pathway for communication. In terms of performance, the BD-RIS surpasses the STAR RIS by an average of 49.15%, the Random Phase scheme by 138.04%, the Random Power scheme by 104.08%, and the TD RIS by 78.55%. Subsequent analyses in Fig. 5 utilized identical simulation parameters as previously mentioned, with adjustments made to the transmit power ranging from 20 dBm to 40 dBm. The findings reveal that with the increment in transmit power at each base station, the BD-RIS maintains superior performance compared to alternative approaches.

Subsequently, results depicted in Fig. 6 demonstrate the influence of SINR, equivalent to with QoS requirements, on the efficacy of the proposed strategies. Observations reveal

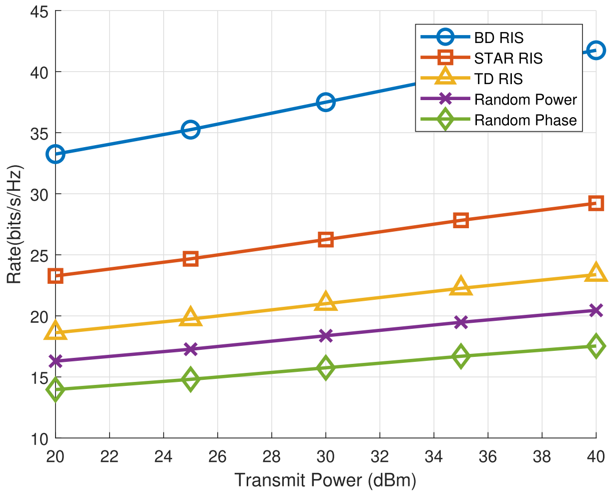

Fig. 6. Transmit power versus the achievable rate of the proposed transportation system.

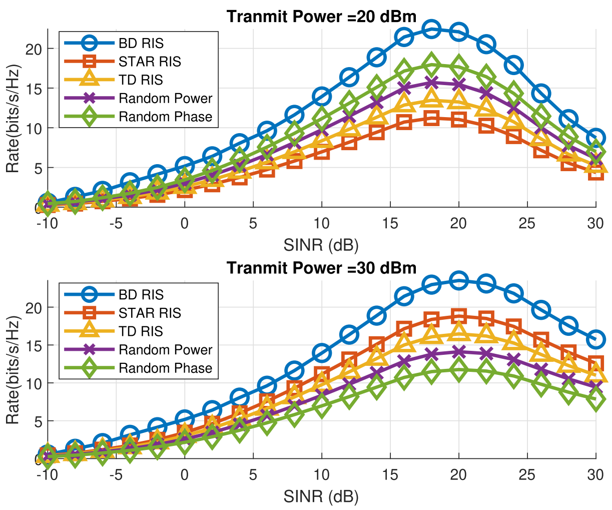

Fig. 7. Spectral efficiency of BD-RIS, STAR-RIS, TD-RIS, random power, and random phase at 20 dBm and 30 dBm transmit power across SINR levels.

that with a fixed transmit power of 20 dBm, as SINR values increase, the system's rate improves until SINR attains 15 dBm. Beyond this point, further increases in SINR result in diminished system performance, leading to decreased overall effectiveness. Nevertheless, this adverse effect can be alleviated by increasing the transmit power to 30 dBm. Furthermore, the results suggest that our proposed strategy surpasses competing schemes, even at lower SINR levels, and this advantage persists even at saturation points.

Following this, Figure 7 displays the effects of different SINR values on system efficiency, with settings of a bandwidth of 10 MHz and a total power constraint of 40 dBm. The study spanned a SINR range from -10 dB to 30 dB. These findings were also benchmarked against other relevant schemes, including STAR RIS, Random Phase, Random Power, and TD RIS. The analysis shows that an elevation in SINR boosts system performance, as higher SINR values are linked to enhanced signal quality and diminished interference. Performance-wise, the BD-RIS markedly excels over STAR RIS by an average of 49.15%, Random Phase by 138.04%, Random Power by 104.08%, and TD RIS by 78.55%.

VI. Conclusion

In this work, we have provided a new communication scenario based on the BD-RIS assisted multi-cell transportation system. In particular, a new optimization framework is investigated to maximize the sum rate of the considered transportation system. Our proposed optimization framework has simultaneously optimized the power allocation of BS and phase shift design of BD-RIS in each cell while taking various practical constraints into account. Due to the mixed integer nonlinear nature of the formulated joint problem, we adopted BCD approach to split the optimization into two problems for power transmission and phase shift design. Then, each problem is further transformed into a linear problem before applying a standard convex optimization method for an efficient solution. Numerical results prove that the proposed BD-RIS assisted transportation system achieves a high sum rate compared to the benchmark classical RIS, START RIS, and suboptimal optimization frameworks.

In the future, our work can be explored in many ways. For instance, we can explore the integration of BD-RIS in dynamic vehicular networks with real-time adaptive control to further improve connectivity in highly mobile environments. Additionally, extending BD-RIS to support hybrid modes in both indoor and outdoor scenarios could enhance system versatility in complex urban scenarios. Another promising direction lies in developing robust machine-learning techniques to predict optimal phase shifts and power allocation based on the vehicle's historical data, reducing real-time computation requirements. Furthermore, investigating energy-efficient and hardware-optimized designs for BD-RIS elements would support sustainable deployments, paving the way for scalable implementations in smart city networks.

References

[1] Y. Liu, L. Huo, J. Wu, and A. K. Bashir, "Swarm learning-based dynamic optimal management for traffic congestion in 6G-driven intelligent transportation system," *IEEE Trans. Intell. Transp. Syst.*, vol. 24, no. 7, pp. 7831–7846, Jul. 2023.

[2] H. Wang, F. H. Memon, X. Wang, X. Li, N. Zhao, and K. Dev, "Machine learning-enabled MIMO-FBMC communication channel parameter estimation in IIoT: A distributed CS approach," *Digit. Commun. Netw.*, vol. 9, no. 2, pp. 306–312, Apr. 2023.

[3] Q. Pan, J. Wu, J. Nebhen, A. K. Bashir, Y. Su, and J. Li, "Artificial intelligence-based energy efficient communication system for intelligent reflecting surface-driven VANETs," *IEEE Trans. Intell. Transp. Syst.*, vol. 23, no. 10, pp. 19714–19726, Oct. 2022.

[4] H. Wang, P. Xiao, and X. Li, "Channel parameter estimation of mmWave MIMO system in urban traffic scene: A training channel-based method," *IEEE Trans. Intell. Transp. Syst.*, vol. 25, no. 1, pp. 754–762, Jan. 2024.

[5] W. U. Khan et al., "Opportunities for physical layer security in UAV communication enhanced with intelligent reflective surfaces," *IEEE Wireless Commun.*, vol. 29, no. 6, pp. 22–28, Dec. 2022.

[6] M. Ahmed et al., "Active reconfigurable intelligent surfaces: Expanding the frontiers of wireless communication—A survey," *Proc. IEEE Commun. Surveys Tuts.*, early access, Jul. 4, 2024, doi: 10.1109/COMST.2024.3423460.

[7] M. Ahmed et al., "A survey on STAR-RIS: Use cases, recent advances, and future research challenges," *IEEE Internet Things J.*, vol. 10, no. 16, pp. 14689–14711, Aug. 2023.

[8] H. Wang, L. Xu, Z. Yan, and T. A. Gulliver, "Low-complexity MIMO-FBMC sparse channel parameter estimation for industrial big data communications," *IEEE Trans. Ind. Informat.*, vol. 17, no. 5, pp. 3422–3430, May 2021.

[9] Y. Liu et al., "Reconfigurable intelligent surfaces: Principles and opportunities," *IEEE Commun. Surveys Tuts.*, vol. 23, no. 3, pp. 1546–1577, 3rd Quart., 2021.

[10] J. Wang et al., "Reconfigurable intelligent surface: Power consumption modeling and practical measurement validation," *IEEE Trans. Commun.*, vol. 72, no. 9, pp. 5720–5734, Sep. 2024.

[11] W. U. Khan et al., "Integration of NOMA with reflecting intelligent surfaces: A multi-cell optimization with SIC decoding errors," *IEEE Trans. Green Commun. Netw.*, vol. 7, no. 3, pp. 1554–1565, Sep. 2023.

[12] D. Gürgünoğlu, E. Björnson, and G. Fodor, "Combating inter-operator pilot contamination in reconfigurable intelligent surfaces assisted multi-operator networks," *IEEE Trans. Commun.*, vol. 72, no. 9, pp. 5884–5895, Sep. 2024.

[13] H. Li, S. Shen, M. Nerini, and B. Clerckx, "Reconfigurable intelligent surfaces 2.0: Beyond diagonal phase shift matrices," *IEEE Commun. Mag.*, vol. 62, no. 3, pp. 102–108, Mar. 2024.

[14] M. Nerini, S. Shen, H. Li, and B. Clerckx, "Beyond diagonal reconfigurable intelligent surfaces utilizing graph theory: Modeling, architecture design, and optimization," *IEEE Trans. Wireless Commun.*, vol. 23, no. 8, pp. 9972–9985, Aug. 2024.

[15] A. Mahmood, T. X. Vu, W. Ullah Khan, S. Chatzinotas, and B. Ottersten, "Joint computation and communication resource optimization for beyond diagonal UAV-IRS empowered MEC networks," 2023, *arXiv:2311.07199*.

[16] W. U. Khan, A. Mahmood, M. A. Jamshed, E. Lagunas, M. Ahmed, and S. Chatzinotas, "Beyond diagonal RIS for 6G non-terrestrial networks: Potentials and challenges," *IEEE Netw.*, early access, Oct. 14, 2024, doi: 10.1109/MNET.2024.3480332.

[17] M. Soleymani, I. Santamaria, E. A. Jorswieck, and B. Clerckx, "Optimization of rate-splitting multiple access in beyond diagonal RIS-assisted URLLC systems," *IEEE Trans. Wireless Commun.*, vol. 23, no. 5, pp. 5063–5078, May 2024.

[18] H. Li, S. Shen, and B. Clerckx, "Beyond diagonal reconfigurable intelligent surfaces: A multi-sector mode enabling highly directional full-space wireless coverage," *IEEE J. Sel. Areas Commun.*, vol. 41, no. 8, pp. 2446–2460, Aug. 2023.

[19] I. Santamaria, M. Soleymani, E. Jorswieck, and J. Gutiérrez, "SNR maximization in beyond diagonal RIS-assisted single and multiple antenna links," *IEEE Signal Process. Lett.*, vol. 30, pp. 923–926, 2023.

[20] Y. Zhou, Y. Liu, H. Li, Q. Wu, S. Shen, and B. Clerckx, "Optimizing power consumption, energy efficiency, and sum-rate using beyond diagonal RIS—A unified approach," *IEEE Trans. Wireless Commun.*, vol. 23, no. 7, pp. 7423–7438, Jul. 2024.

[21] Z. Liu, Y. Liu, S. Shen, Q. Wu, and Q. Shi, "Enhancing ISAC network throughput using beyond diagonal RIS," *IEEE Wireless Commun. Lett.*, vol. 13, no. 6, pp. 1670–1674, Jun. 2024.

[22] H. Li, S. Shen, and B. Clerckx, "Synergizing beyond diagonal reconfigurable intelligent surface and rate-splitting multiple access," *IEEE Trans. Wireless Commun.*, vol. 23, no. 8, pp. 8717–8729, Aug. 2024.

[23] H. Zhao, W. Sun, Y. Ni, W. Xia, G. Gui, and C. Zhu, "Deep deterministic policy gradient-based rate maximization for RIS-UAV-assisted vehicular communication networks," *IEEE Trans. Intell. Transp. Syst.*, vol. 25, no. 11, pp. 15732–15744, Nov. 2024.

[24] M. Wu, Y. Xiao, Y. Gao, and M. Xiao, "Digital twin for UAV-RIS assisted vehicular communication systems," *IEEE Trans. Wireless Commun.*, vol. 23, no. 7, pp. 7638–7651, Jul. 2024.

[25] B. Ji et al., "Vehicular communication based on RIS-assisted source: RIS-relay versus energy harvesting relay," *IEEE Trans. Intell. Transp. Syst.*, early access, Oct. 23, 2024, doi: 10.1109/TITS.2024.3479692.

[26] B. Ji, S. Wang, G. Zhang, J. Liu, and S. Mumtaz, "Performance analysis of RIS-assisted V2V communication under multipath interference," *Veh. Commun.*, vol. 45, Feb. 2024, Art. no. 100696.

[27] P. Shang et al., "Secure index modulation for RIS-aided vehicle road cooperation networks," *IEEE Internet Things J.*, vol. 11, no. 22, pp. 35864–35876, Nov. 2024.

[28] L. Chen, J. Zhu, Y. Yang, and S. Boichenko, "Physical-layer security for RIS-V2V networks with different eavesdropper locations," *IEEE Internet Things J.*, vol. 11, no. 22, pp. 35791–35801, Nov. 2024.

[29] B. Ji et al., "Performance analysis of RIS-enhanced secure transmission for symbiotic IoV systems," *IEEE Trans. Cognit. Commun. Netw.*, early access, Aug. 12, 2024, doi: 10.1109/TCCN.2024.3431925.

[30] H. Li, S. Shen, and B. Clerckx, "Beyond diagonal reconfigurable intelligent surfaces: From transmitting and reflecting modes to single-, group-, and fully-connected architectures," *IEEE Trans. Wireless Commun.*, vol. 22, no. 4, pp. 2311–2324, Apr. 2023.

[31] M. Nerini, S. Shen, and B. Clerckx, "Closed-form global optimization of beyond diagonal reconfigurable intelligent surfaces," *IEEE Trans. Wireless Commun.*, vol. 23, no. 2, pp. 1037–1051, Feb. 2024.

[32] H. Li, S. Shen, M. Nerini, M. Di Renzo, and B. Clerckx, "Beyond diagonal reconfigurable intelligent surfaces with mutual coupling: Modeling and optimization," *IEEE Commun. Lett.*, vol. 28, no. 4, pp. 937–941, Apr. 2024.

[33] W. Sun, S. Sun, T. Shi, X. Su, and R. Liu, "A new model of beyond diagonal reconfigurable intelligent surfaces (BD-RIS) for the corresponding quantization and optimization," *IEEE Trans. Wireless Commun.*, vol. 23, no. 9, pp. 11521–11534, Sep. 2024.

[34] A. Mishra, Y. Mao, C. D'Andrea, S. Buzzi, and B. Clerckx, "Transmitter side beyond-diagonal reconfigurable intelligent surface for massive MIMO networks," *IEEE Wireless Commun. Lett.*, vol. 13, no. 2, pp. 352–356, Feb. 2024.

[35] Z. Guang, Y. Liu, Q. Wu, W. Wang, and Q. Shi, "Power minimization for ISAC system using beyond diagonal reconfigurable intelligent surface," *IEEE Trans. Veh. Technol.*, vol. 73, no. 9, pp. 13950–13955, Sep. 2024.

[36] T. Fang and Y. Mao, "A low-complexity beamforming design for beyond-diagonal RIS aided multi-user networks," *IEEE Commun. Lett.*, vol. 28, no. 1, pp. 203–207, Jan. 2024.

[37] Q. Li, M. El-Hajjar, I. Hemadeh, A. Shojaeifard, and L. Hanzo, "Coordinated reconfigurable intelligent surfaces: Non-diagonal group-connected design," *IEEE Trans. Veh. Technol.*, vol. 73, no. 7, pp. 10811–10816, Jul. 2024.

[38] M. Deng et al., "Reconfigurable intelligent surfaces enabled vehicular communications: A comprehensive survey of recent advances and future challenges," *IEEE Trans. Intell. Vehicles*, early access, Oct. 14, 2024, doi: 10.1109/TIV.2024.3476934.

[39] W. U. Khan, F. Jameel, X. Li, M. Bilal, and T. A. Tsiftsis, "Joint spectrum and energy optimization of NOMA-enabled small-cell networks with QoS guarantee," *IEEE Trans. Veh. Technol.*, vol. 70, no. 8, pp. 8337–8342, Aug. 2021.

[40] W. U. Khan, M. A. Jamshed, E. Lagunas, S. Chatzinotas, X. Li, and B. Ottersten, "Energy efficiency optimization for backscatter enhanced NOMA cooperative V2X communications under imperfect CSI," *IEEE Trans. Intell. Transp. Syst.*, vol. 24, no. 11, pp. 12961–12972, Nov. 2023.

[41] W. U. Khan, E. Lagunas, A. Mahmood, S. Chatzinotas, and B. Ottersten, "RIS-assisted energy-efficient LEO satellite communications with NOMA," *IEEE Trans. Green Commun. Netw.*, vol. 8, no. 2, pp. 780–790, Jun. 2024.

[42] A. Mahmood, T. X. Vu, W. U. Khan, S. Chatzinotas, and B. Ottersten, "Optimizing computational and communication resources for MEC network empowered UAV-RIS communication," in *Proc. IEEE Globecom Workshops (GC Wkshps)*, Rio de Janeiro, Brazil, Apr. 2022, pp. 974–979.

[43] X. Mu, Y. Liu, L. Guo, J. Lin, and R. Schober, "Simultaneously transmitting and reflecting (STAR) RIS aided wireless communications," *IEEE Trans. Wireless Commun.*, vol. 21, no. 5, pp. 3083–3098, May 2021.